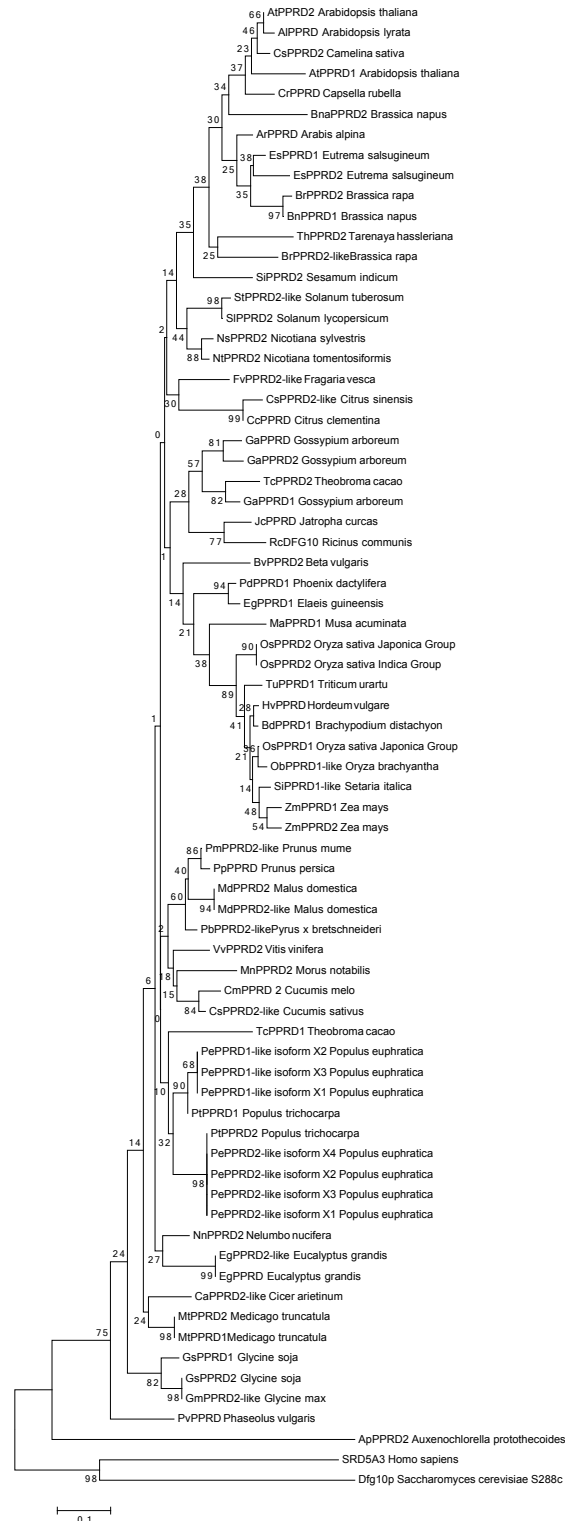
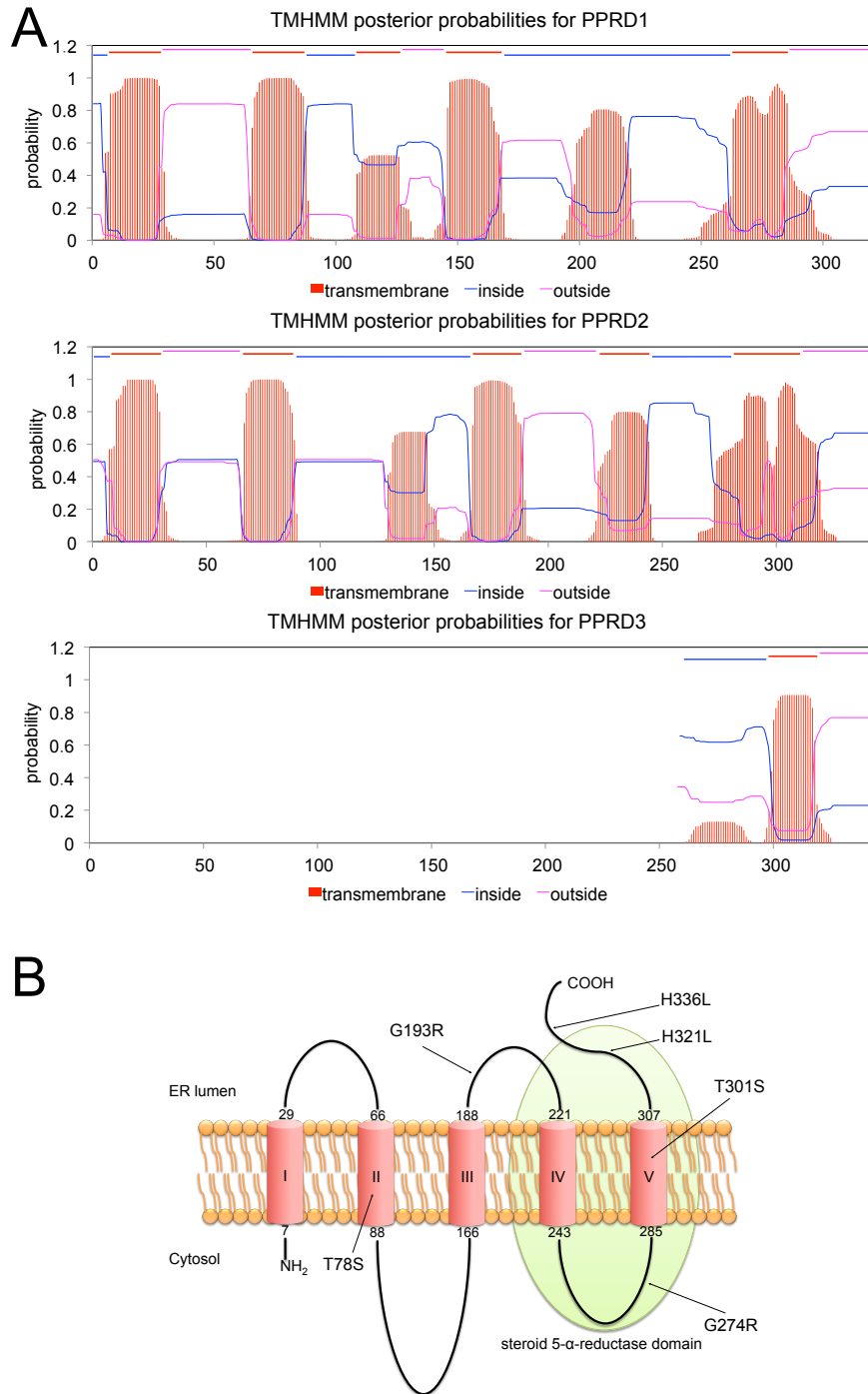


**Supplemental Figure 1.** Alignment of Amino Acid Sequences of Proteins with Steroid 5 $\alpha$ -Reductase Domain from Human (hSRD5A3), Yeast *Saccharomyces cerevisiae* (Dfg10p) and 60 Plant Species. Highly conserved amino acids are highlighted. The alignment was made using the ClustalW program. Related to Figure 1.

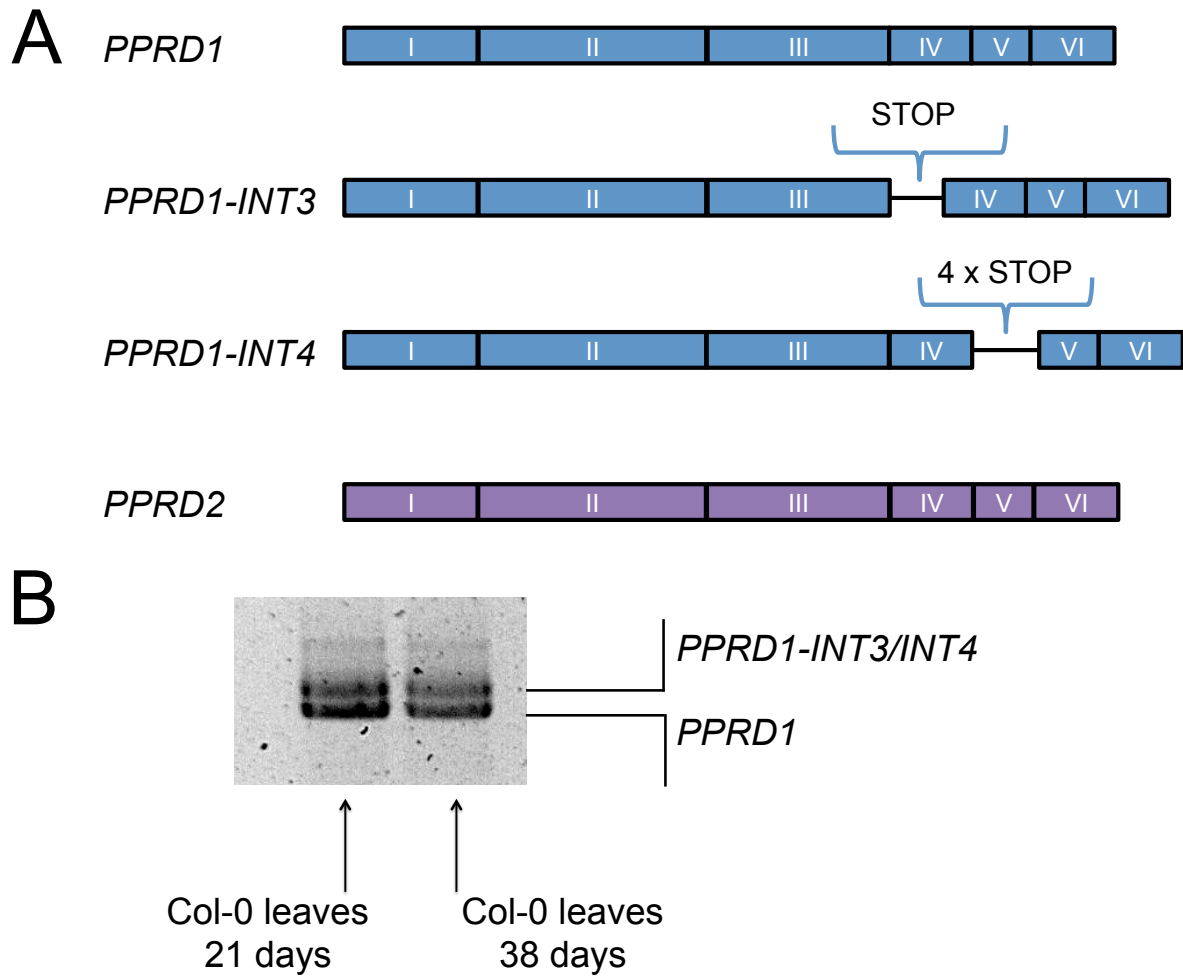


**Supplemental Figure 2.** Evolutionary Tree of Proteins with Steroid 5 $\alpha$ -Reductase Domain. Amino acid sequences of proteins from 60 plant species, yeast (Dfg10p) and human (hSRD5A3) were aligned as above and the tree was constructed using the neighbor-joining method. Related to Supplemental Figure 1.



**Supplemental Figure 3. Models of PPRDs, Related to Supplemental Figure 1.**

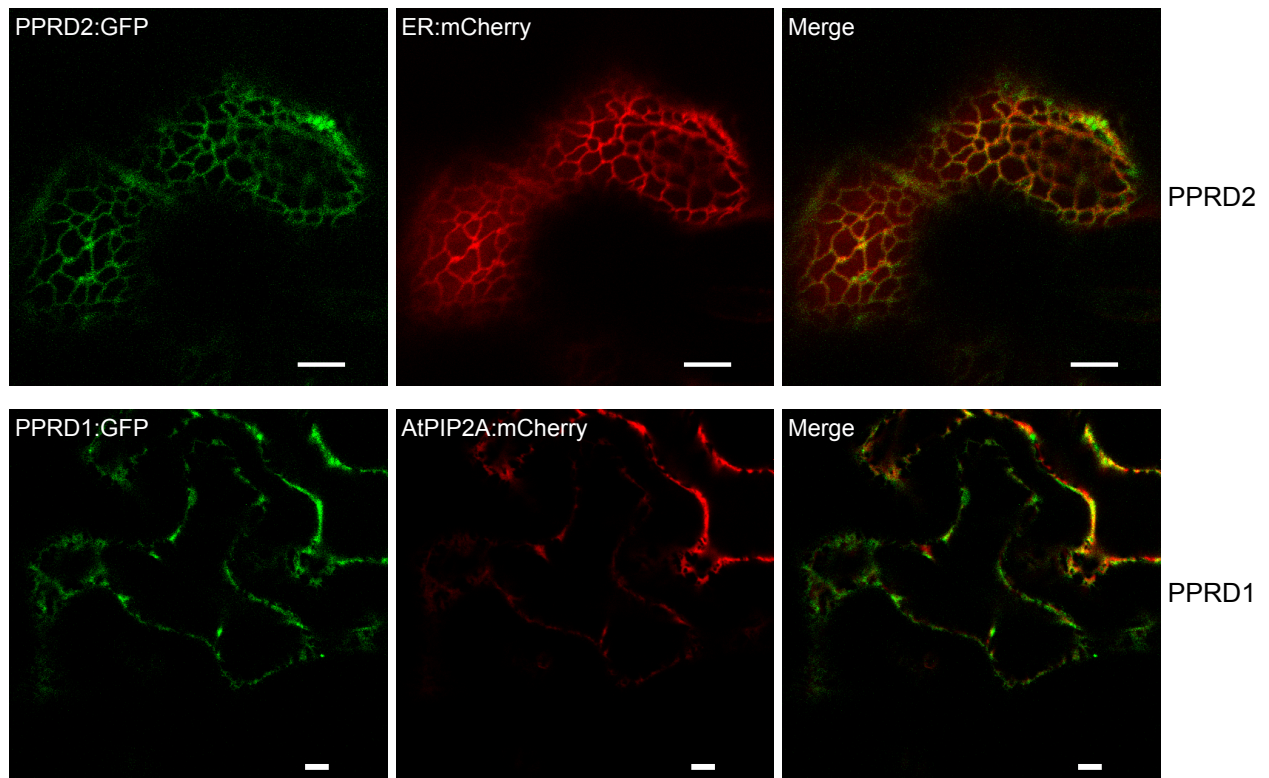
(A) Predicted transmembrane domains in PPRD1, PPRD2 and PPRD3. Please note that numbering of X-axis used for PPRD3 does not align to the amino acid numbers in this protein. (B) Topology model of PPRD2; five predicted transmembrane domains (in red) and putative steroid reductase domain (in green) are indicated. Amino acid residues of particular interest are indicated, namely H321 and H336 subjected to site-directional mutagenesis (this report) and natural polymorphisms observed for PPRD2 isolated from *Arabidopsis thaliana* hairy roots (T78S, G193R, G274R and T301S).



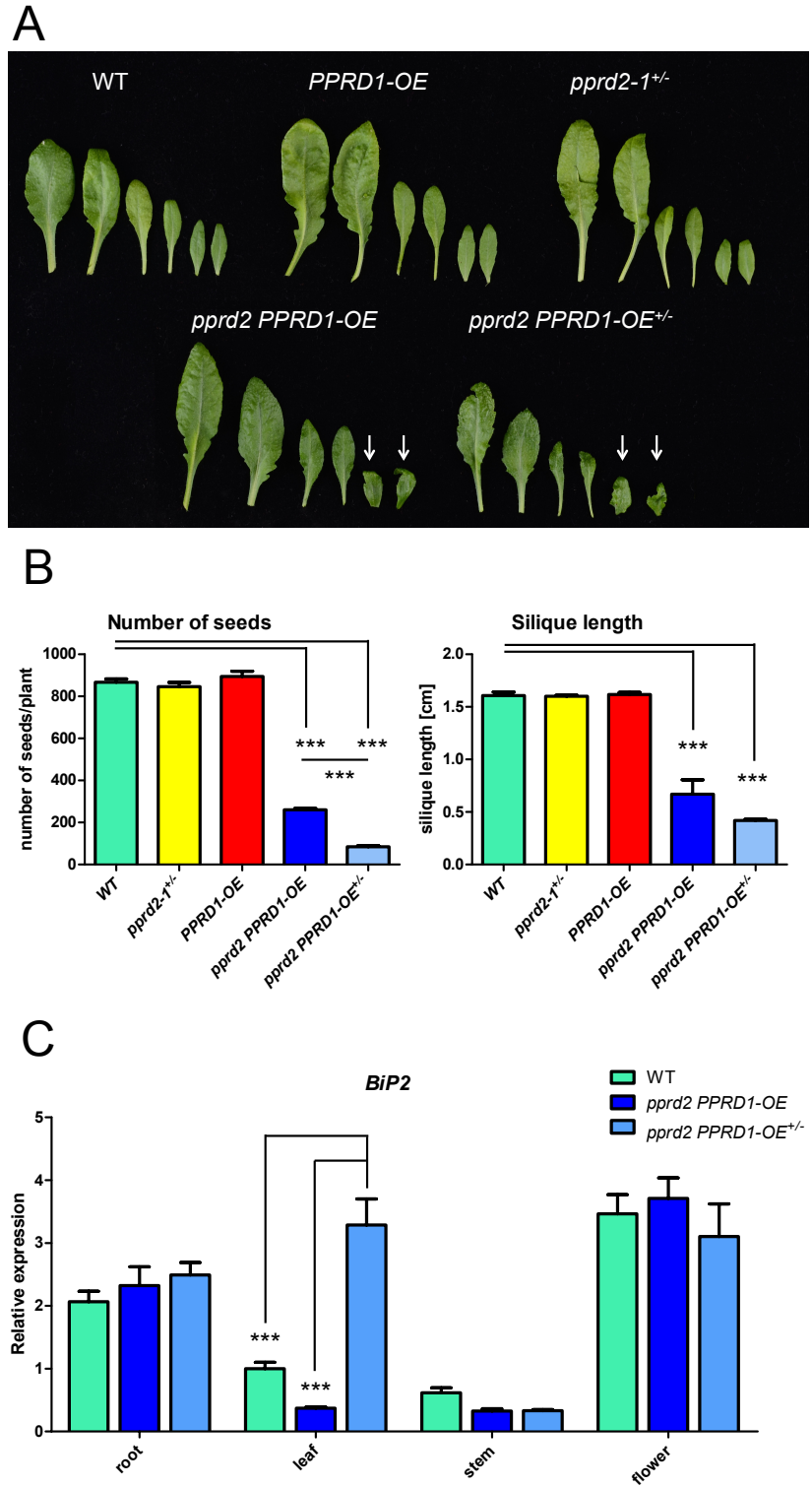
**Supplemental Figure 4.** Schematic Representation and Expression of PPRDs, Related to Figure 2.

(A) Structure of coding sequences of *PPRD1*, *PPRD1-INT3*, *PPRD1-INT4* and *PPRD2*. Premature STOP codons are present in *PPRD1-INT3* and *PPRD1-INT4*. The two latter DNA fragments were obtained during cloning of *PPRD1* cDNA.

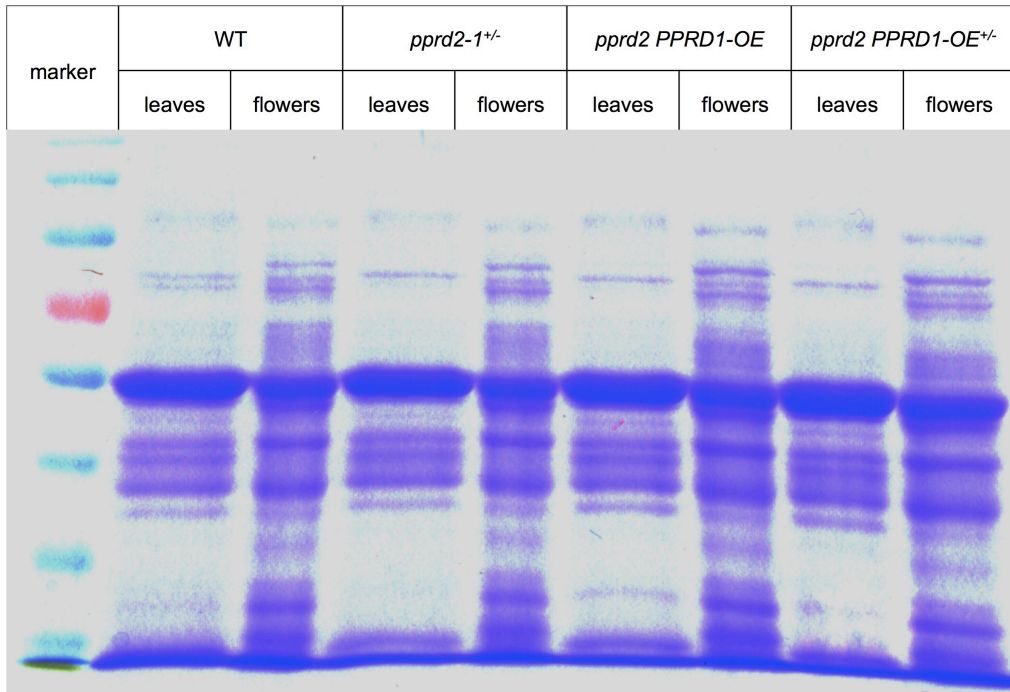
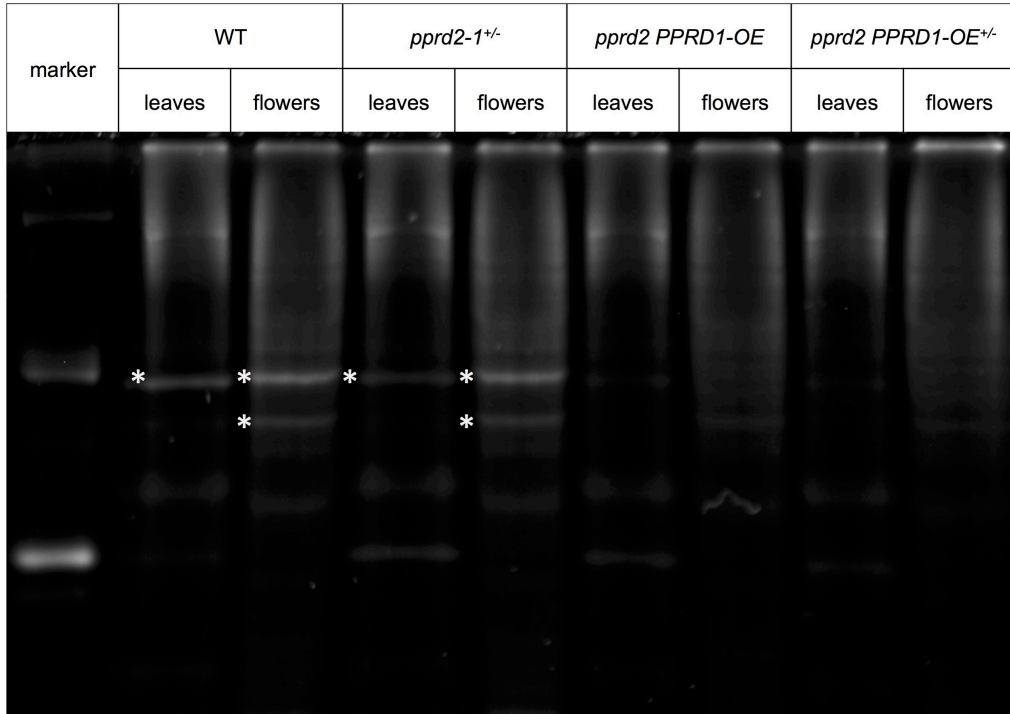
(B) *PPRD1* transcripts detected by (RT-PCR) in the leaves of 21- and 38-day-old WT plants. Bands corresponding to *PPRD1* and *PPRD1-INT3/PPRD1-INT4* are indicated.



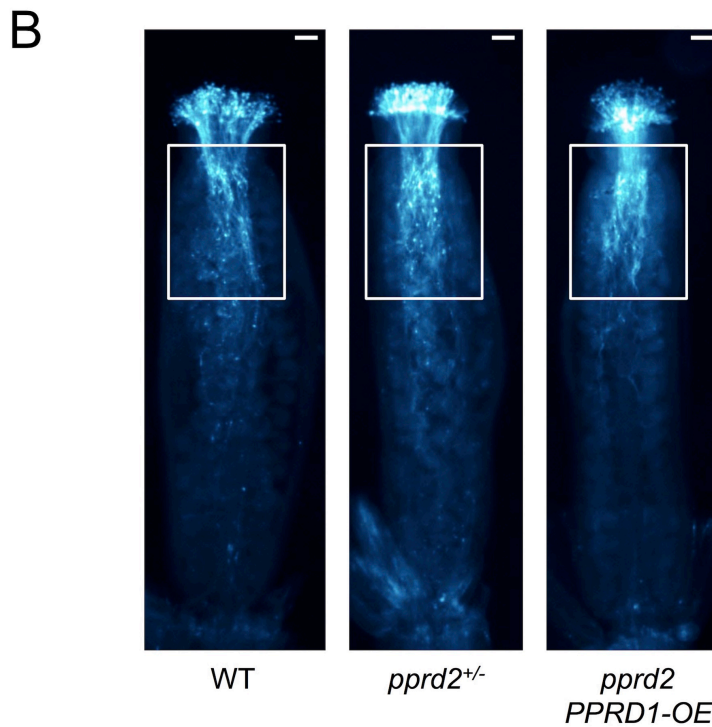
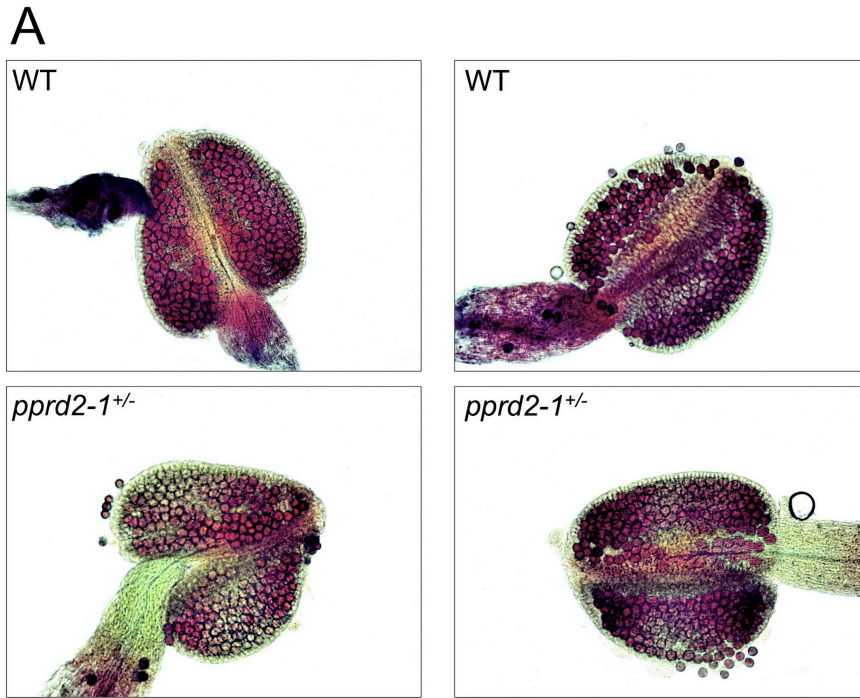
**Supplemental Figure 5. Subcellular Localization of PPRD1 and PPRD2. Related to Figure 2.** Co-localization of GFP-tagged PPRD2 or PPRD1 (green) with organelle markers – ER:mCherry and AtPIP2A:mCherry (red). Scale bar = 10  $\mu$ m.



**Supplemental Figure 6.** Phenotypes of WT, *pprd2-1<sup>+/-</sup>*, *PPRD1-OE*, *pprd2 PPRD1-OE* and *pprd2 PPRD1-OE<sup>+/-</sup>* Plants. Related to Figure 4. (A) Leaves, (B) seed number and silique length and (C) expression of *BiP2* in WT and studied mutants. White arrows indicate undulated leaves. Statistically significant differences from WT are indicated; \*\*\* -  $P < 0.001$ .



**Supplemental Figure 7. Analysis of Glycosylated Proteins in WT, *pprd2-1<sup>+/-</sup>*, *pprd2 PPRD1-OE* and *pprd2 PPRD1-OE<sup>+/-</sup>* Plants.** Protein extracts from leaves and flowers were separated by SDS-PAGE and gel was stained with Glycoprotein Gel Stain (upper image) or Coomassie Brilliant Blue (lower image). Marker lines contain, respectively, Glycoprotein Molecular Weight Standard or PageRuler™ Prestained Protein Marker. Asterisks mark bands present in WT extracts but absent in *pprd2* lines.

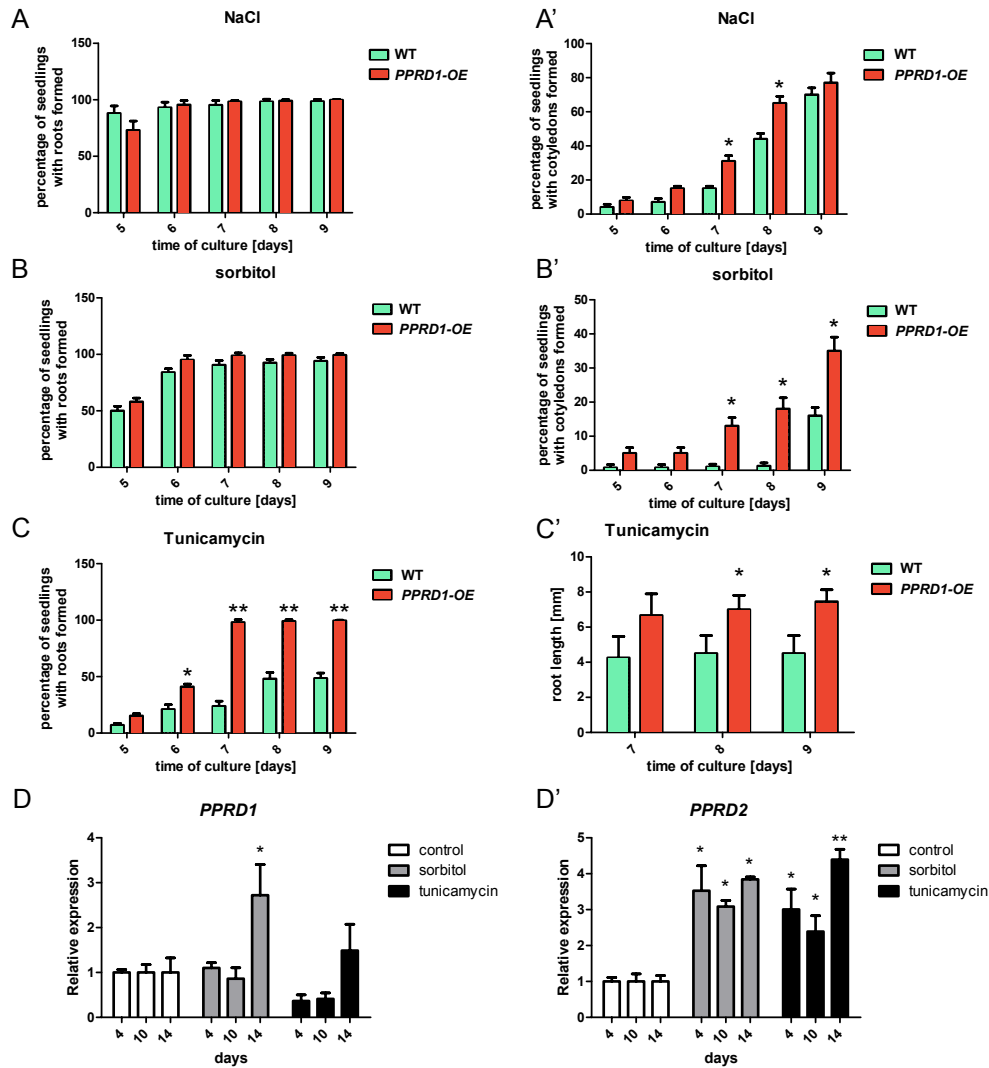


**Supplemental Figure 8. (A) Alexander Staining of Mature Anthers of WT and *pprd2-1<sup>+/-</sup>* Plants and (B) Aniline Blue Staining of Pollen Tube in the Pistil.**

For the latter analysis pollen grains from wild-type, *pprd2<sup>+/-</sup>* or *pprd2* PPRD1-OE mutants were used to pollinate wild-type stigma. Pollen tubes were visualized by aniline blue staining. White frame indicates region of highest accumulation of inhibited pollen tubes of mutant origin. Scale bar = 100  $\mu$ m.

Related to Figure 5 and 6.





**Supplemental Figure 9. Effect of *PPRD1* Overexpression on Plant Tolerance to Stress.**

Effect of sodium chloride and sorbitol (A, B) and tunicamycin (C) on WT and *PPRD1-OE* seed germination. Percentage of seedlings with roots formed (A, B, C); cotyledons (A', B') and root growth (C'). Fifty seeds of each genotype were germinated per experiment; values are means  $\pm$  SD of three independent experiments. (D) Expression of *PPRD1* (D) and *PPRD2* (D') in *Arabidopsis* seedlings treated with sorbitol or tunicamycin normalized to control conditions. Bars represent mean value  $\pm$ SD of four independent experiments. Statistically significant differences are indicated; \* -  $P < 0.05$  and \*\* -  $P < 0.01$ .

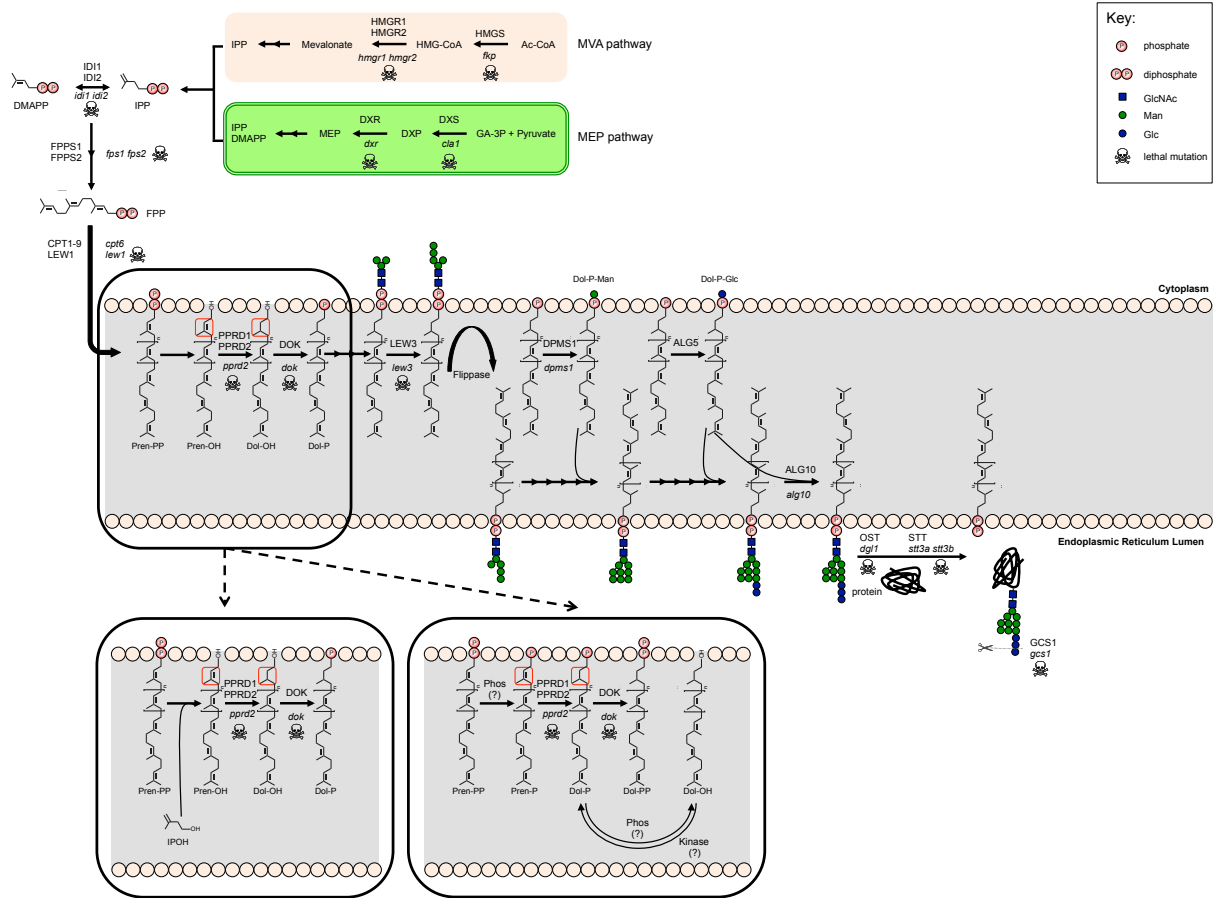
Since dolichol is postulated to participate in cell response to environmental stress *PPRD1-OE* plants (Figure 3B) containing higher Dol level (Figure 3E) were challenged with various stimuli. Therefore the plant germination test was performed in the presence of sorbitol or NaCl.

Overexpression of *PPRD1* improved the formation of cotyledons upon NaCl and especially sorbitol treatments, while it did not affect the appearance of roots comparing to WT plants (Panels A/A' and Panels B/B').

Additionally, effect of tunicamycin, an inhibitor of protein glycosylation on seed germination was tested too. Overexpression of *PPRD1* enabled development of roots for all the seedlings in contrast to WT plants (only 50% of germinating seeds). Moreover the roots of the *PPRD1-OE* seedling were substantially longer than WT (Panels C/C'). Thus, overexpression of *PPRD1* increases plant tolerance to sorbitol and salinity and prevents tunicamycin toxicity.

To study further the relations between the PPRDs and stress we determined their expression profiles in WT plants treated with sorbitol and tunicamycin (Panels D/D'). *PPRD2* expression was induced 3-4-fold after four days of treatment with either compound and increased slightly with time. In contrast, the *PPRD1* expression was induced 3-fold by sorbitol after fourteen days and somewhat inhibited by tunicamycin during ten days of treatment.

Taken together, *PPRD2* undergoes induction in response to various adverse environmental factors.



**Supplemental Figure 10. Dolichol Cycle in Plant Cells, Related to Discussion.**

Genes crucial for the pathway are indicated, lethal phenotypes are marked. Two insets present alternative, yet not documented steps of Prenol to Dolichol conversion. Abbreviations used: MVA - mevalonate, Ac-CoA - acetyl-CoA, GA-3P - D-glyceraldehyde-3-phosphate, HMG-S - 3-hydroxy-3-methylglutaryl-CoA synthase, HMG-CoA - 3-hydroxy-3-methylglutaryl-coenzyme A, HMGGR - 3-hydroxy-3-methylglutaryl-CoA reductase, IPP - isopentenyl diphosphate, DMAPP - dimethylallyl diphosphate, DXS - 1-deoxy-D-xylulose-5-phosphate synthase, DXR - 1-deoxy-D-xylulose 5-phosphate reductoisomerase, DXP - 1-deoxy-D-xylulose 5-phosphate, MEP - 2-C-methylerythritol 4-phosphate, IDI - isopentenyl diphosphate isomerase, FPPS - farnesyl diphosphate synthase, CPT - *cis*-prenyltransferase, PPRD – polyprenol reductase, DOK – dolichol kinase, LEW - leaf wilting, DPMS - DolPMan synthase, ALG5 - putative dolichyl-phosphate beta-glucosyltransferase, ALG10 - alpha-1,2-glucosyltransferase, OST - dolichyl-diphosphooligosaccharide-protein glycosyltransferase, STT - dolichyl-diphosphooligosaccharide-protein glycosyltransferase, GCS - alpha-glucosidase 2, Phos – phosphatase.

**Supplemental Table 1.** Comparison of Amino Acid Sequences of Putative PPRDs with Human and Yeast Polyprenol Reductases Based on the Alignment, Related to Supplemental Figure 1.

Protein	Gene locus	Comparison to hSRD5A3			Comparison to Dfg10p		
		Identity [%]	Similarity [%]	BLASTP E-value	Identity [%]	Similarity [%]	BLASTP E-value
PPRD1	At1G72590	29	50	8E-36	26	39	2E-15
PPRD2	At2G16530	28	47	3E-38	27	42	2E-13
PPRD3	At3G43840	30	54	0.031	27	47	1E-04

**Supplemental Table 2.** Localisation of Predicted 3-oxo-5- $\alpha$ -steroid 4-dehydrogenase Domain in Arabidopsis Polyprenol Reductases. Related to Supplemental Figure 3.

Protein	Protein length [a.a.]	Predicted 3-oxo-5- $\alpha$ -steroid 4-dehydrogenase domain [a.a.]	E-value
PPRD1	320	199-320	7.2E-24
PPRD2	343	223-343	1.1E-22
PPRD3	84	14-84	6.7E-10

**Supplemental Table 3.** Seed Germination of *pprd2-1<sup>+/-</sup>* and *pprd2-2<sup>+/-</sup>* Plants on Solid Medium, Related to Figure 4.

Seeds	<i>pprd2-1<sup>+/-</sup></i>	<i>pprd2-2<sup>+/-</sup></i>	WT
Sown	203 (100%)	210 (100%)	200 (100%)
Germinated	197 (97%)	206 (98%)	198 (99%)

**Supplemental Table 4.** Mass Spectrometry-based Differential Proteomics of WT and *pprd2 PPRD1-OE<sup>+/-</sup>* Plants. Proteins extracted from the flowers of 10-week-old plants were subjected to MS analysis. Listed are the proteins present in WT but totally absent from *pprd2 PPRD1-OE<sup>+/-</sup>*. Predicted number of *N*-glycosylation sites, function (described / predicted) and site of expression of particular proteins according to NetNGlyc 1.0 Server and TAIR database, respectively.

No.	Protein	Predicted glycosylation sites	Gene locus	Function	Expressed in (organs with highest expression are in bold)
1	ASN2, ASPARAGINE SYNTHETASE 2	2	AT5G65010	L-asparagine biosynthetic process, ammonium ion metabolic process, asparagine biosynthetic process, cysteine biosynthetic process, glutamine metabolic process, hyperosmotic salinity response	carpel, cauline leaf, collective leaf structure, <b>cotyledon</b> , flower, guard cell, <b>hypocotyl</b> , inflorescence meristem, leaf apex, leaf lamina base, pedicel, petal, petiole, plant embryo, plant sperm cell, pollen tube cell, root, seed, sepal, shoot apex, shoot system, stamen, stem, <b>vascular leaf</b>
2	GLYCOSYL HYDROLASE FAMILY PROTEIN	4	AT5G20950	carbohydrate metabolic process, glucan catabolic process, response to endoplasmic reticulum stress, systemic acquired resistance	adult vascular leaf, <b>carpel</b> , cauline leaf, collective leaf structure, cotyledon, flower, fruit, guard cell, hypocotyl, <b>inflorescence meristem</b> , juvenile vascular leaf, leaf apex, leaf lamina base, pedicel, petal, petiole, plant embryo, pollen, root, seed, sepal, <b>shoot apex</b> , shoot system, stamen, stem, vascular leaf
3	ABNORMAL INFLORESCEN CE MERISTEM, AIM1	3	AT4G29010	fatty acid beta-oxidation, flower development, jasmonic acid biosynthetic process, multicellular organismal development, seed germination	carpel, cauline leaf, collective leaf structure, cotyledon, <b>flower</b> , fruit, guard cell, hypocotyl, inflorescence meristem, leaf apex, leaf lamina base, pedicel, <b>petal</b> , petiole, plant embryo, pollen, root, <b>seed</b> , sepal, shoot apex, shoot system, <b>stamen</b> , stem, vascular leaf
4	PECTIN LYASE-LIKE SUPERFAMILY PROTEIN	7	AT4G23500	carbohydrate metabolic process, cell wall organization	guard cell, <b>inflorescence meristem</b>
5	SKS11, SKU5 SIMILAR 11	6	AT3G13390	oxidation-reduction process	carpel, collective leaf structure, flower, pedicel, petal, plant embryo, pollen, <b>pollen</b> tube cell, sepal, <b>stamen</b> , stem
6	A. THALIANA	1	AT3G10160	one-carbon metabolic process,	carpel, cauline leaf, collective leaf structure,

	DHFS-FPGS HOMOLOG C, DFC			photorespiration, seedling development, tetrahydrofolylpolyglutamate biosynthetic process	cotyledon, <b>flower</b> , guard cell, hypocotyl, <b>inflorescence meristem</b> , leaf apex, leaf lamina base, pedicel, petal, petiole, plant embryo, pollen, root, <b>seed</b> , sepal, <b>shoot apex</b> , shoot system, stamen, stem, <b>vascular leaf</b>
7	Transducin/WD 40 repeat-like superfamily protein	2	AT2G20330	N-terminal protein myristoylation, biological_process, photoperiodism, flowering, protein targeting to mitochondrion	carpel, cauline leaf, collective leaf structure, cotyledon, cultured plant cell, flower, guard cell, hypocotyl, <b>inflorescence meristem</b> , leaf apex, leaf lamina base, pedicel, petal, petiole, <b>plant embryo</b> , plant sperm cell, pollen, pollen tube cell, root, <b>seed</b> , sepal, <b>shoot apex</b> , shoot system, stamen, stem, vascular leaf
8	HOP1	2	AT1G12270	cullin deneddylation, nucleotide biosynthetic process, photomorphogenesis	<b>carpel</b> , cauline leaf, collective leaf structure, cotyledon, cultured plant cell, <b>flower</b> , guard cell, hypocotyl, <b>inflorescence meristem</b> , <b>leaf apex</b> , leaf lamina base, pedicel, <b>petal</b> , petiole, plant embryo, pollen, <b>root</b> , <b>seed</b> , sepal, <b>shoot apex</b> , shoot system, stamen, stem, vascular leaf
9	O-Glycosyl hydrolases family 17 protein	8	AT1G11820	carbohydrate metabolic process, defense response	guard cell, <b>inflorescence meristem</b>
10	HDA5, HISTONE DEACETYLASE 5	1	AT5G61060	fatty acid beta-oxidation, histone deacetylation, protein N-linked glycosylation, protein import into peroxisome matrix, regulation of transcription, DNA-templated, transcription, DNA-templated	<b>carpel</b> , <b>cauline leaf</b> , collective leaf structure, cotyledon, <b>flower</b> , guard cell, hypocotyl, <b>inflorescence meristem</b> , leaf apex, leaf lamina base, pedicel, <b>petal</b> , petiole, plant embryo, pollen, root, seed, sepal, shoot apex, shoot system, stamen, stem, vascular leaf
11	PCK1, PEPCK, PHOSPHOENO LPYRUVATE CARBOXYKINA SE	2	AT4G37870	cellular response to phosphate starvation, defense response to fungus, incompatible interaction, gluconeogenesis, response to cadmium ion	<b>carpel</b> , cauline leaf, collective leaf structure, cotyledon, cultured plant cell, <b>flower</b> , guard cell, hypocotyl, <b>inflorescence meristem</b> , leaf apex, leaf lamina base, pedicel, <b>petal</b> , petiole, <b>plant embryo</b> , plant sperm cell, pollen, root, rosette leaf, <b>seed</b> , sepal, shoot apex, shoot system, stamen, <b>stem</b> , vascular leaf
12	1-DEOXY-D- XYLULOSE 5-	5	AT4G15560	1-deoxy-D-xylulose 5-phosphate biosynthetic process, aromatic amino	<b>carpel</b> , <b>cauline leaf</b> , <b>cotyledon</b> , epidermis, flower, fruit, guard cell, hypocotyl, <b>inflorescence</b>

	PHOSPHATE SYNTHASE, CLA, DXS,			acid family biosynthetic process, aromatic amino acid family metabolic process, carotenoid biosynthetic process, cell differentiation, cellular amino acid biosynthetic process, chlorophyll biosynthetic process, chlorophyll metabolic process, coenzyme biosynthetic process, cysteine biosynthetic process, glycine catabolic process, isopentenyl diphosphate biosynthetic process, methylerythritol 4-phosphate pathway, jasmonic acid biosynthetic process, leaf morphogenesis, lipoate metabolic process, nucleotide metabolic process, oxidoreduction coenzyme metabolic process, oxylipin biosynthetic process, phosphatidylglycerol biosynthetic process, positive regulation of transcription, DNA-templated, protein autophosphorylation, regulation of lipid metabolic process, regulation of protein localization, regulation of proton transport, response to light stimulus, secondary metabolic process, sulfur amino acid metabolic process, sulfur compound biosynthetic process, thiamine biosynthetic process, vitamin metabolic process	<b>meristem</b> , leaf apex, leaf lamina base, pedicel, <b>petal</b> , petiole, plant embryo, pollen, root, seed, sepal, <b>shoot apex</b> , shoot system, stamen, stem, stigma, trichome, <b>vascular leaf</b>
13	PAL4, PHENYLALANINE AMMONIOLYASE 4	3	AT3G10340	L-phenylalanine catabolic process, cinnamic acid biosynthetic process, glucuronoxytan metabolic process, xylan biosynthetic process	carpel, collective leaf structure, <b>flower</b> , guard cell, hypocotyl, inflorescence meristem, <b>petal</b> , petiole, <b>plant embryo</b> , pollen, root, sepal, shoot apex, shoot system, <b>stamen</b> , vascular leaf
14	ABCF3	2	AT1G64550	cytoskeleton organization, defense response to bacterium,	<b>carpel</b> , cauline leaf, collective leaf structure, cotyledon, cultured plant cell, <b>flower</b> , guard cell,



				gluconeogenesis, glycolytic process, mRNA export from nucleus, proteasomal protein catabolic process, protein import into nucleus, response to cadmium ion, response to salt stress	hypocotyl, <b>inflorescence meristem</b> , leaf apex, leaf lamina base, pedicel, petal, petiole, plant embryo, pollen, root, <b>seed</b> , sepal, <b>shoot apex</b> , shoot system, stamen, stem, vascular leaf
15	GH3.17	1	AT1G28130	auxin homeostasis, brassinosteroid biosynthetic process, response to auxin	carpel, collective leaf structure, <b>flower</b> , hypocotyl, <b>petal</b> , plant embryo, pollen, root, seed, sepal, shoot apex, shoot system, <b>stamen</b> , stem, vascular leaf
16	AN, ANGUSTIFOLIA	2	AT1G01510	actin nucleation, cell adhesion, chromatin silencing, floral organ morphogenesis, fruit morphogenesis, histone H3-K9 methylation, histone phosphorylation, inductive cell-cell signaling, leaf morphogenesis, microtubule cytoskeleton organization, monopolar cell growth, oxidation-reduction process, regulation of cell shape, regulation of epidermal cell differentiation, regulation of epidermal cell division, regulation of trichome morphogenesis, trichome branching, trichome morphogenesis	<b>carpel</b> , cauline leaf, collective leaf structure, cotyledon, <b>flower</b> , guard cell, hypocotyl, <b>inflorescence meristem</b> , leaf apex, leaf lamina base, pedicel, petal, petiole, <b>plant embryo</b> , pollen, <b>root</b> , seed, sepal, <b>shoot apex</b> , shoot system, stamen, stem, vascular leaf

**Methodology:** Peptide mixtures were analyzed by liquid chromatography coupled to an LTQ FT ICR mass spectrometer (Hybrid-2D-Linear Quadrupole Ion Trap – Fourier Transform Ion Cyclotron Resonance Mass Spectrometer, Thermo Electron Corp., Bremen, Germany). Gel slices were subjected to a standard digestion procedure, during which proteins were reduced with 100 mM DTT for 30 min at 56°C, alkylated with iodoacetamide for 45 min in a darkroom at 22°C and digested overnight with Trypsin. The resulting peptides were eluted from the gel with 0.1% TFA and 2% ACN. The peptide mixture was applied to an RP-18 pre-column (LC Packings) using water that contained 0.1% TFA as the mobile phase and then transferred to a nano-HPLC RP-18 column (nanoACQUITY UPLC BEHC18, Waters) using an acetonitrile gradient (0–60% ACN in 30 min) in the presence of 0.05% formic acid with a flow rate of 150 nL/min. The column outlet was directly coupled to an ion source of LTQ-FT-MS that worked in the regime of data dependent MS to MS/MS switch. A blank run that ensured a lack of cross-contamination from previous samples preceded each analysis.

Acquired raw data were processed by Mascot Distiller (version 2.1.1, Matrix Science, London, UK) followed by Mascot Search database search engine (v.2.1, Matrix Science).

**Supplemental Table 5.** Effect of Polyprenol, Dolichol and Tunicamycin on Pollen Germination on Solid Medium, Related to Figure 6. Statistically significant differences are indicated: \* -  $P < 0.05$ ; \*\*\* -  $P < 0.001$ 

	Regular medium		Medium supplemented with						
			Prenol-16		Dolichol - MIX		Tunicamucin, WT pollen		
							0 ng/ml n=164	10 ng/ml n=203	50 ng/ml n=241
Pollen grains	WT, n=1208	<i>pprd2-1<sup>+/-</sup></i> , n=1424	WT, n=482	<i>pprd2-1<sup>+/-</sup></i> , n=438	WT, n=522	<i>pprd2-1<sup>+/-</sup></i> , n=508			
normal	1160 (96%)	812 (57%)	458 (95%)	228 (52%)	506 (97%)	488 (96%)	161 (98%)	171 (84%)	94 (39%)
deformed	48 (4%)	612 (43%)***	24 (5%)	210 (48%)***	16 (3%)	20 (4%)	3 (2%)	32 (16%)*	147 (61%)*

**Supplemental Table 6.** Phenotypes of Arabidopsis Mutants in Genes Encoding Elements of Isoprenoid Synthesis or Protein Glycosylation Pathways, Related to Discussion.

Gene	Function	Phenotype	Reference
<b>MVA pathway encoding genes</b>			
<i>HMGS</i>	3-hydroxy-3-methylglutaryl-CoA synthase	<i>fkp</i> (flaky pollen) null mutant is lethal due to male-sterility; <i>fkp1-4</i> pollen, carrying null allele of the gene, has normal 3 nuclei as visualized by DAPI stain, but does not germinate normally and is 100% sterile; weak <i>fkp1-1</i> allele does not affect the vegetative growth, but pollen grains formed on heterozygote are infertile due to abnormal development of tapetum-specific organelles - elaioplasts and tapetosomes - leading to reduced pollen coat deposition and, as a consequence, adhesion and hydration on stigma	Ishiguro et al., 2010
<i>HMGR1</i> <i>HMGR2</i>	3-hydroxy-3-methylglutaryl-CoA reductase responsible for formation of mevalonate	<i>hmgr1 hmgr2</i> double mutant is lethal due to male-sterility; <i>hmgr1<sup>+/-</sup> hmgr2</i> heterozygous plants - half of pollen grains are malformed, shrunken and have underdeveloped ER structures, pollen lethality is due to both gametophytic and maternal sporophytic effects; <i>hmgr1</i> single mutant - plants are dwarfed and homozygotes are male sterile, short empty siliques are formed, male sterility comes from sporophytic, maternal defect of tapetum and can be reversed by external application of squalene, but not brassinosteroids on inflorescence	Suzuki et al., 2009  Suzuki et al., 2004
<i>IDI1</i> <i>IDI2</i>	isopentenyl diphosphate isomerase responsible for formation of dimethylallyl diphosphate	<i>idi1 idi2</i> double mutant is lethal due to male-sterility	Phillips et al., 2008
<b>MEP pathway encoding genes</b>			
<i>DXS</i>	1-deoxy-D-xylulose 5-phosphate synthase	<i>cla1</i> mutant is albino lethal; chloroplast biogenesis is affected	Mandel et al., 1996 Budziszewski et al., 2001
<i>DXR</i>	1-deoxy-D-xylulose 5-phosphate reducto-	<i>dxr</i> mutant is albino lethal; chloroplast biogenesis is affected	Budziszewski et al., 2001 Xing et al.,

	isomerase		2010
<b>Isoprenoid chain formation</b>			
<i>FPPS1</i> <i>FPPS2</i>	farnesyl diphosphate synthase responsible for synthesis of FPP	<i>fps1 fps2</i> double mutant is lethal due to block on embryo development at pre-globular stage, transmission through male gametophyte is severely reduced (12% of expected frequency), pollen grains develop 3 nuclei, pollen germination is not impaired, but growth of pollen tube is severely affected; <i>fps1</i> and <i>fps2</i> single mutants are viable and show minor biochemical defects;	Closa et al., 2010
<i>CPT1-9</i> 2 out of 9 putative genes characterized	<i>cis</i> -prenyltransferase responsible for formation of polyprenyl diphosphate (syn. dehydrodolichyl diphosphate)	<i>cpt6</i> single mutant does not show phenotypic aberrations	Surmacz et al., 2014
<i>LEW1</i>	described as atypical AtCPT recently recognized as AtCPT-like accessory protein (ortholog of hNogoBR)	<i>lew1</i> null mutant is lethal	Zhang et al., 2008 Qu et al., 2015
<i>PPRD1</i> <i>PPRD2</i>	polyprenol reductase responsible for conversion of polyprenol to dolichol	<i>pprd2</i> null mutation is lethal due to nonfunctional pollen, transmission through male gametophyte is abolished; <i>pprd2</i> point mutations - no defect observed; <i>pprd2</i> <sup>+/-</sup> heterozygous plant – sporophyte does not show phenotypic changes, approx. 50% pollen grains are wrinkled and pollen tubes are malformed	this report
<i>DOK</i>	dolichol kinase responsible for formation of dolichyl phosphate	<i>dok (evn)</i> null mutation is lethal, both mutated pollen and female gametophytes are nonfunctional; <i>dok</i> <sup>+/-</sup> heterozygous plant pollen is infertile, suggesting that intrinsic rather than maternal effect contributes to the lethality, mutated pollen grains wrinkled and hollow, some ovules have aberrant morphology and probably are unable to be fertilized	Kanehara et al., 2015 Lindner et al., 2015
<b>Protein glycosylation pathway</b>			
<i>DPMS1</i>	catalytic subunit of DoIPMan	<i>dpms1</i> mutant is viable, possesses wrinkled seed coat and is hypersensitive to	Jadid et al., 2011

	synthase responsible for mannosylation of DoIP	ammonium (chlorosis and strong reduction of root growth)	
<i>ALG1</i>	beta-1,4-mannosyltransferase responsible for transfer of mannose to DoIPP-GlcNAc <sub>2</sub>	<i>tun</i> null mutant is lethal due to defects in pollen tube reception.	Lindner et al., 2015
<i>LEW3</i>	alfa-1,2-mannosyltransferase responsible for mannosylation of DoIPP-GlcNAc <sub>2</sub> Man <sub>3</sub>	<i>lew3</i> null mutant is lethal; <i>lew3</i> point mutant shows reduced fertility, short siliques, impaired cellulose synthesis, abnormal primary and secondary cell wall biosynthesis	Zhang et al., 2009
<i>ALG10</i>	alfa-1,2-glucosyltransferase responsible for the terminal glucosylation of DoIPP-GlcNAc <sub>2</sub> Man <sub>9</sub> Glc <sub>2</sub> precursor	<i>alg10-1</i> mutant is viable, displays severe protein underglycosylation, reduced leaf size, reduced tolerance to salt stress	Farid et al., 2011
multigene OST complex	oligosaccharide transferase complex responsible for transfer of tetradecasaccharide structure from DoIP-GlcNAc <sub>2</sub> Man <sub>9</sub> Glc <sub>3</sub> to protein (Asn-X-Ser/Thr)	<i>dgl1-2</i> null mutant in one of OST complex subunits is embryo-lethal; <i>dgl1-1</i> point mutant shows developmental defects in early seedling development, including reduced cell elongation and collapse of cells of central cylinder due to changes in accumulation of callose; <i>stt3a stt3b</i> double mutant in OST complex subunit is gametophytic lethal	Lerouxel et al., 2005;  Koiwa et al., 2003
<i>GCS1</i>	glycan trimming after oligosaccharide transfer onto Asn in a protein molecule	<i>gcs1</i> mutant is embryo-lethal (heart stage of development) and shows abnormal cell enlargement and occasional cell wall disruptions, abnormal accumulation of seed storage proteins, cytokinesis and cellulose biosynthesis	Boisson et al., 2001
<i>N</i> - glycan processing of <i>N</i> -glycosylated	subsequent downstream steps of <i>N</i> -glycan	homozygous null mutants show abnormalities in root growth, aberrant cellulose deposition pattern	Liebmingier et al., 2009; Schaewen et al., 1993;

proteins	processing		Strasser et al., 2004; Strasser et al., 2004b; Strasser et al., 2006; Strasser et al., 2007
<i>SETH1</i> <i>SETH2</i>	first step of GPI biosynthetic pathway	<i>seth1</i> and <i>seth2</i> mutations block male transmission and pollen function due to reduced pollen germination and tube growth, abnormal callose deposition	Lalanne et al., 2004
<i>APTG1</i>	mannosyltransferase involved in GPI-anchor biosynthesis	<i>aptg1</i> (abnormal pollen tube guidance) mutant pollen tubes shows compromised micropylar guidance, embryo lethality	Dai et al., 2014
<i>PNT1</i>	mannosyltransferase involved in GPI-anchor biosynthesis	<i>pnt1</i> mutants are embryo-lethal, at early stages show large reduction in crystalline cellulose and an increase in pectin content, ectopic deposition of xyloglucan, pectin, and callose, poor transmission through pollen, with no significant effect on egg transmission	Gillmor et al., 2005

**Supplemental Table 7.** Primers Used for Genotyping, Cloning, Mutagenesis and Expression Studies, Related to Materials and Methods.

Genotyping primers		
Gene	Allele	Primer sequence
<i>PPRD1</i>	<i>PPRD1-OE</i>	gFP1 F: 5'-CATATTTATAGTGTGGGGTGGC-3' gRP1 R: 5'-GAAAGAGAAAACGTGGGAACC-3'
<i>PPRD2</i>	<i>pprd2-1</i>	gFP2 F: 5'-GTCTGTGAATTTGCCCATCTG-3' gRP2 R: 5'-TCCA CT CGCAATCAGTAAACC-3'
	<i>pprd2-2</i>	gFP2 F: 5'-GTCTGTGAATTTGCCCATCTG-3' gRP2 R: 5'-TCCA CT CGCAATCAGTAAACC-3'
LBb1.3	-	5'-ATTTTGCCGATTTCCGGAAC-3'
qPCR primers		
Gene	Locus	Primer sequence
<i>PPRD1</i>	At1g72590	qFP1 F: 5'-GTGGCTGCTAATCTGACATAC-3' qRP1 R: 5'-GTATAA ACTTGGCCAAAGTTGTG-3'
<i>PPRD2</i>	At2g16530	qFP2 F: 5'-GTGGCTGCTAATCTGACATAC-3' qRP2 R: 5'-CAGCATTACAGAAGACAACCA-3'
<i>BiP2</i>	At5g42020	F: 5'-GGTATCGAGACTGTAGGAGG-3' R: 5'-GGTACGTTGTGAAAACCTGA-3'
<i>ACTIN-2</i>	At3g18780	F: 5'-GACCAGCTCTTCCATCGAGAA-3' R: 5'-CAAACGAGGGCTGGAACAAG-3'
Cloning primers		
Gene	Tag type	Primer sequence
<i>PPRD1</i>	No tag	F: 5'-CACCATGGAGGTAGAGATTGTGTGG-3' R: 5'-TTAGTAGACATGAGGGAAAATAGCATGC-3'
	GST	F: 5'-CACCATGGAGGTAGAGATTGTGTGG-3' R: 5'-GTAGACATGAGGGAAAATAGCATGC-3'
<i>PPRD2</i>	No tag	F: 5'-CACCATGGTGG AATTGGAGATTGTG-3' R: 5'-TTAGTAGACATAAGGGAAAATGGCATGC-3'
	GST	F: 5'-CACCATGGTGG AATTGGAGATTGTG-3' R: 5'-GTAGACATAAGGGAAAATGGCATGCC-3'
<i>PPRD1<sub>Pro</sub></i>	nd	F: 5'-CACCTTCTTATATAAAAATAAGGTAAAGGAAGAATAT-3' R: 5'-CTCCATACTTTTTTTTTTTTGTGTGTGTGTG-3'
<i>PPRD2<sub>Pro</sub></i>	nd	F: 5'-CACCAAGGCATAACTTAATAACAAGCTCCACTA-3' R: 5'-ACTTTTTTGT TTAGTGT TTTCTTCTCTGAAATC-3'
Mutagenesis primers		
Construct	Primer sequence	
<i>PPRD2 H321L</i>	F: 5'-CACCATGGTGG AATTGGAGATTGTG-3' R: 5'-CGTTTCTCCAGCCGCGTATGTCAGATTAGC-3' F: 5'-TCTGACATACGCGGCTGGAGAAACGCTCCG-3' R: 5'-TTAGTAGACATAAGGGAAAATGGCATGC-3'	
<i>PPRD2 H336L</i>	F: 5'-CACCATGGTGG AATTGGAGATTGTG-3' R: 5'-TTAGTAGACATAAGGGAAAATGGCAAGCC-3'	